



American Society of Hematology
 2021 L Street NW, Suite 900,
 Washington, DC 20036
 Phone: 202-776-0544 | Fax 202-776-0545
 editorial@hematology.org

ABBV-319: A CD19-targeting glucocorticoid receptor modulator antibody-drug conjugate therapy for B-cell malignancies

Tracking no: BLD-2024-023849R2

Chewei Chang (AbbVie Inc., United States) Ethan Emberley (AbbVie Inc., United States) Aloma D'Souza (AbbVie Inc., United States) Weilong Zhao (AbbVie Inc., United States) Cormac Cosgrove (AbbVie Inc., United States) Karen Parrish (AbbVie Inc., United States) Diya Mitra (AbbVie Inc., United States) Elmer Payson (AbbVie Inc., United States) Anatol Oleksijew (AbbVie Inc., United States) Paul Ellis (AbbVie Inc., United States) Luis Rodriguez (AbbVie Inc., United States) Ryan Duggan (AbbVie Inc., United States) Cara Hrusch (AbbVie Inc., United States) Loren Lasko (AbbVie Inc., United States) Wissam Assaily (AbbVie Inc., United States) Pingping Zheng (AbbVie Inc., United States) Wei Liu (AbbVie Inc., United States) Axel Hernandez (AbbVie Inc., United States) Kimberley McCarthy (AbbVie Inc., United States) Zhaomei Zhang (AbbVie Inc., United States) Geunbae Rha (AbbVie Inc., United States) Zhensheng Cao (AbbVie Inc., United States) Yingchun Li (AbbVie Inc., United States) Olivia Perng (AbbVie Inc., United States) Jos Campbell (AbbVie Inc., United States) Gloria Zhang (AbbVie Inc., United States) Tyler Curran (AbbVie Inc., United States) Milan Bruncko (AbbVie Inc., United States) Christopher Marvin (AbbVie Inc., United States) Adrian Hobson (AbbVie Inc., United States) Michael McPherson (AbbVie Inc., United States) Tamar Uziel (AbbVie Inc., United States) Marybeth Pysz (AbbVie Inc., United States) Xi Zhao (AbbVie Inc., United States) Alexander Bankovich (Link Cell Therapies, Inc, United States) Joel Hayflick (AbbVie Inc., United States) Michael McDevitt (AbbVie Inc., United States) Kevin Freise (AbbVie Inc., United States) Susan Morgan-Lappe (AbbVie Inc., United States) James Purcell (AbbVie Inc., United States)

Abstract:

Glucocorticoids are key components of the current standard-of-care regimens (e.g., R-CHOP, EPOCH-R, Hyper-CVAD) for treatment of B-cell malignancy. However, systemic glucocorticoid treatment is associated with several adverse events. CD19 displays restricted expression in normal B-cells and is up-regulated in B-cell malignancies. ABBV-319 is a CD19-targeting antibody-drug conjugate (ADC) engineered to reduce glucocorticoid-associated toxicities while possessing three distinct mechanisms of action (MOA) to increase therapeutic efficacy: (1) antibody-mediated delivery of glucocorticoid receptor modulator (GRM) payload to activate apoptosis, (2) inhibition of CD19 signaling, and (3) enhanced Fc-mediated effector function via afucosylation of the antibody backbone. ABBV-319 elicited potent GRM-driven anti-tumor activity against multiple malignant B-cell lines in vitro as well as in cell line-derived xenografts (CDXs) and patient-derived xenografts (PDXs) in vivo. Remarkably, a single-dose of ABBV-319 induced sustained tumor regression and enhanced anti-tumor activity compared to repeat dosing of systemic prednisolone at the maximum tolerated dose (MTD) in mice. The unconjugated CD19 monoclonal antibody (mAb) also displayed anti-proliferative activity on a subset of B-cell lymphoma cell lines through the inhibition of PI3K signaling. Moreover, afucosylation of the CD19 mAb enhanced Fc-mediated antibody-dependent cellular cytotoxicity (ADCC), and this activity was maintained after conjugation with GRM payloads. Notably, ABBV-319 displayed superior efficacy compared to afucosylated CD19 mAb in human CD34+ PBMC-engrafted NSG-tg(Hu-IL15) transgenic mice, demonstrating enhanced anti-tumor activity when multiple MOAs are enabled. ABBV-319 also showed durable anti-tumor activity across multiple B-cell lymphoma PDX models, including non-germinal center B-cell (GCB) DLBCL and relapsed lymphoma post R-CHOP treatment. Collectively, these data support the ongoing evaluation of ABBV-319 in Phase I clinical trial (NCT05512390).

Conflict of interest: COI declared - see note

COI notes: CAC, EE, ALD, WZ, CC, KP, DM, EP, AO, PE, LR, RD, CH, LL, WA, PZ, WL, AHJ, KM, ZZ, GR, ZC, YL, JC, GZ, TC, MB, CCM, AH, MM, TU, MAP, XZ, JH, MM, KF, SML, and JWP are employees of AbbVie. OP and AB were employees of AbbVie at the time of the study. The design, study conduct, and financial support for this research were provided by AbbVie. AbbVie participated in the interpretation of data, review, and approval of the publication.

Preprint server: No;

Author contributions and disclosures: Conception and design: CAC, EE, AD, WZ, TU, JWP Acquisition of data: CAC, AD, CC, DM, EP, AO, PE, LR, CH, LL, WA, PZ, AH, KM, ZZ, GR, ZC, OP, JC Analysis and interpretation of data (e.g., statistical analysis, biostatistics, computational analysis): CAC, EE, AD, WZ, CC, DM, RD, AH, KM, TU, JWP Writing, review, and/or revision of the manuscript: CAC wrote the manuscript and all authors reviewed the manuscript prior to submission.

Non-author contributions and disclosures: No;

Agreement to Share Publication-Related Data and Data Sharing Statement: The RNA-seq and CITE-seq data are available at GEO under accession number GSE249023 and GSE249543, respectively.

Clinical trial registration information (if any):

1 **Title:** ABBV-319: A CD19-targeting glucocorticoid receptor modulator antibody-drug conjugate
2 therapy for B-cell malignancies

3
4 **Authors:** Chewei Anderson Chang¹, Ethan Emberley¹, Aloma L. D'Souza¹, Weilong Zhao¹,
5 Cormac Cosgrove², Karen Parrish², Diya Mitra², Elmer Payson¹, Anatol Oleksijew², Paul Ellis²,
6 Luis Rodriguez², Ryan Duggan², Cara Hrusch², Loren Lasko², Wissam Assaily¹, Pingping Zheng¹,
7 Wei Liu¹, Axel Hernandez Jr³, Kimberley McCarthy³, Zhaomei Zhang¹, Geunbae Rha², Zhensheng
8 Cao², Yingchun Li², Olivia Perng¹, Jos Campbell¹, Gloria Zhang¹, Tyler Curran¹, Milan Bruncko²,
9 Christopher C. Marvin², Adrian Hobson³, Michael McPherson³, Tamar Uziel², Marybeth A. Pysz¹,
10 Xi Zhao¹, Alex Bankovich¹, Joel Hayflick¹, Michael McDevitt¹, Kevin J. Freise², Susan Morgan-
11 Lappe², James W. Purcell¹

12
13 **Affiliations:** ¹AbbVie Bay Area, 1000 Gateway Boulevard, South San Francisco, CA 94080;
14 ²AbbVie Inc., 1 North Waukegan Rd., North Chicago, IL 60064; ³AbbVie Bioresearch Center, 100
15 Research Drive, Worcester, MA 01605

16
17 **Short Title for Running Head:** Preclinical Study of ABBV-319 for B-cell Malignancies

18
19 **Corresponding Authors:**

20 Chewei Anderson Chang
21 AbbVie, Inc.
22 Oncology Discovery Research
23 1000 Gateway Blvd
24 South San Francisco
25 CA 94080
26 Email: anderson.chang@abbvie.com
27 Phone: +1 650-540-6560

28
29 James Purcell
30 AbbVie Inc.
31 Oncology Discovery Research
32 1000 Gateway Blvd
33 South San Francisco
34 CA 94080
35 Email: james.purcell@abbvie.com
36 Phone: +1-650-540-6604

37
38 The RNA-seq and CITE-seq data are available at GEO under accession number GSE249023 and
39 GSE249543, respectively.

40
41 **Abstract word count:** 250 of maximum 250 words

42 **Word count (Introduction, Methods, Results and Discussion):** 3935 of maximum 4000 words

43 **Figure count:** 7 of maximum 7 figures

44 **References count:** 42 of maximum 100 references

45

46 **Data Sharing Statement:** The RNA-seq and CITE-seq data are available at GEO under accession
47 number GSE249023 and GSE249543, respectively.

48 **Key Point**

49 ABBV-319 is a CD19-targeting GRM ADC with three mechanisms that contribute to pronounced
50 anti-tumor activity across B-cell malignancy models.

51

52 **Abstract**

53 Glucocorticoids are key components of the current standard-of-care regimens (*e.g.*, R-CHOP,
54 EPOCH-R, Hyper-CVAD) for treatment of B-cell malignancy. However, systemic glucocorticoid
55 treatment is associated with several adverse events. CD19 displays restricted expression in
56 normal B-cells and is up-regulated in B-cell malignancies. ABBV-319 is a CD19-targeting
57 antibody-drug conjugate (ADC) engineered to reduce glucocorticoid-associated toxicities while
58 possessing three distinct mechanisms of action (MOA) to increase therapeutic efficacy: (1)
59 antibody-mediated delivery of glucocorticoid receptor modulator (GRM) payload to activate
60 apoptosis, (2) inhibition of CD19 signaling, and (3) enhanced Fc-mediated effector function via
61 afucosylation of the antibody backbone. ABBV-319 elicited potent GRM-driven anti-tumor
62 activity against multiple malignant B-cell lines *in vitro* as well as in cell line-derived xenografts
63 (CDXs) and patient-derived xenografts (PDXs) *in vivo*. Remarkably, a single-dose of ABBV-319
64 induced sustained tumor regression and enhanced anti-tumor activity compared to repeat
65 dosing of systemic prednisolone at the maximum tolerated dose (MTD) in mice. The
66 unconjugated CD19 monoclonal antibody (mAb) also displayed anti-proliferative activity on a
67 subset of B-cell lymphoma cell lines through the inhibition of PI3K signaling. Moreover,
68 afucosylation of the CD19 mAb enhanced Fc-mediated antibody-dependent cellular cytotoxicity
69 (ADCC), and this activity was maintained after conjugation with GRM payloads. Notably, ABBV-

70 319 displayed superior efficacy compared to afucosylated CD19 mAb in human CD34+ PBMC-
71 engrafted NSG-tg(Hu-IL15) transgenic mice, demonstrating enhanced anti-tumor activity when
72 multiple MOAs are enabled. ABBV-319 also showed durable anti-tumor activity across multiple
73 B-cell lymphoma PDX models, including non-germinal center B-cell (GCB) DLBCL and relapsed
74 lymphoma post R-CHOP treatment. Collectively, these data support the ongoing evaluation of
75 ABBV-319 in Phase I clinical trial (NCT05512390).

76

77 **Introduction**

78 Glucocorticoids exhibit clinical activity across B-cell malignancies including diffuse large B-cell
79 lymphoma (DLBCL), chronic lymphocytic leukemia (CLL), follicular lymphoma (FL) and acute
80 lymphoblastic leukemia (ALL).⁶ The anti-tumorigenic effects of glucocorticoids on lymphoma
81 and leukemia were first discovered in clinical studies from the 1950s.^{7,8} Glucocorticoids have
82 demonstrated single-agent and combinatorial anti-tumor activity with different
83 chemotherapeutic agents.^{8,9} Glucocorticoids are thus incorporated into combination regimens
84 for B-cell malignancies, such as R-CHOP (rituximab, cyclophosphamide, doxorubicin, vincristine,
85 prednisone), EPOCH-R (etoposide, prednisone, vincristine, cyclophosphamide, doxorubicin, and
86 rituximab), and hyper CVAD (cyclophosphamide, vincristine, doxorubicin, dexamethasone,
87 methotrexate, and cytarabine). Mechanistically, glucocorticoids act as an agonist for
88 glucocorticoid receptors (GR) to facilitate activation or repression of downstream transcription
89 targets associated with cell cycle progression (e.g., *MYC*, *CCND3*) and apoptosis genes (e.g.,
90 *BCL2L11*, *BCL2*), which subsequently result in cell cycle arrest and/or apoptosis of malignant B-
91 cells.¹¹⁻¹⁴ However, the administration of glucocorticoids systemically is associated with a broad

92 range of potentially dose-limiting side effects such as hyperglycemia, diabetes mellitus,
93 osteoporosis, or psychosis,¹⁵ and these side effects limit the full therapeutic potential of
94 glucocorticoids.

95
96 CD19 is a well-validated therapeutic target for B-cell malignancy including B-cell non-Hodgkin
97 lymphoma (NHL) and leukemia.¹⁶ In normal development, CD19 expression is restricted to the
98 B-cell lineage and its expression increases with B-cell maturation.¹⁷ CD19 is a co-receptor for the
99 B-cell receptor (BCR) and the phosphorylation of its cytoplasmic domain mediates recruitment
100 of phosphoinositide 3-kinase (PI3K), generation of secondary messenger phosphatidylinositol-3,
101 4,5-triphosphate (PIP3), and the activation of downstream signaling molecules including BTK,
102 PLC γ 2, AKT, and mTOR.^{18,19} In B-cell lymphoma and leukemia, CD19 is over-expressed and its
103 expression is often maintained in later-lines, even post CD19-targeting therapies.²⁰⁻²² Moreover,
104 genetic perturbation studies revealed that CD19 plays a critical role in the survival of Burkitt
105 lymphoma (BL) and germinal center B-cell (GCB) like DLBCL cells.²³ Therefore, CD19 is an
106 attractive therapeutic target for the development of biologics and immunotherapy.²⁴

107
108 Here, we describe the preclinical characterization of ABBV-319, a CD19-targeting GRM agonist
109 ADC for the treatment of B-cell malignancy. ABBV-319 elicits anti-tumor activity through three
110 distinct mechanisms of actions (MOAs) that collectively contribute to robust anti-tumor
111 activities across B-cell lymphoma models, including non-GCB DLBCL and PDX samples from
112 relapse/refractory (R/R) lymphoma with poor clinical outcomes.^{4,25} ABBV-319 is currently being
113 investigated in a clinical trial (NCT05512390) as a new therapeutic option for B-cell malignancy.

114
115
116
117
118
119
120
121
122
123
124
125
126
127
128
129
130
131
132
133
134
135

Methods

Antibodies and drug conjugates

CD19 monoclonal antibody (mAb) was discovered at AbbVie and the afucosylated monoclonal antibody (mAb) was generated by heterologous expression of GDP-6-deoxy-D-lyxo-4-hexulose reductase in the Chinese hamster ovary cell line that disrupts the formation of GDP-fucose, and thus preventing addition of fucose to the mAb.

The drug substance process conjugating the mAb and linker-drug includes a phosphine-based redox reaction and a hydrophobic interaction chromatography (HIC) purification that results in a mix of drug-to-antibody ratio (DAR) 2/4/6 distribution with a mean DAR of approximately 4.0, followed by buffer exchange and formulation.

Compounds and formulation

GRM small molecule was synthesized at AbbVie. Dexamethasone (S1322, Selleck Chemicals) and prednisolone (P6004, Sigma-Aldrich) were purchased commercially. The small molecules were dissolved in DMSO for *in vitro* studies and were formulated in 0.05% HPMC, 0.02% Tween-80 in water for *in vivo* studies. Prednisolone sodium phosphate oral solution (44523-0182-08, BioComp Pharma) was used for *in vivo* benchmark studies. All antibodies and ADCs were formulated in appropriate ADC buffer containing lyoprotectant.

Cell lines

136 All cell lines were obtained from ATCC or DSMZ and cultured in growth media supplemented
137 with either fetal bovine serum (FBS; F4135, Sigma-Aldrich) or human serum (HS; H4522, Sigma-
138 Aldrich) at 5% CO₂ at 37°C. Growth media for each cell line is described in supplemental Table 1.

139
140 Detailed protocol for over-expression of CD19 and reporter cell line generation and assays are in
141 the supplemental Methods.

142

143 *In vitro cellular screen*

144 Cells were seeded at 1000 cells/well in 384-well tissue culture plates (Corning) in a total volume
145 of 25 µl in their respective culture media. The plates were dosed the following day with GRM
146 payload, dexamethasone, prednisolone, afucosylated (Af.) isotype mAb, Af. CD19 mAb and
147 ABBV-319 at 0.1 µM, 1 µM, 10 µM, 1 µM, 1 µM and 1 µM top doses, respectively, using ECHO
148 Liquid Handler. Each drug was dosed as a 12-point dilution series with 3-fold dilution between
149 successive concentrations and as triplicates on the same plate per dosing session. Cell
150 proliferation following 120 hours of drug treatment was determined using the Cell Titer-Glo
151 Luminescent Cell Viability Assay kit (Promega) as per manufacturer's recommendation. The EC₅₀
152 and % E_{max} for all drugs with all cell lines are relative to Staurosporine using in-house analysis
153 tools. Median EC₅₀ and %E_{max} from all repeats were reported.

154

155 *RNA sequencing*

156 RNA was isolated from frozen cell pellets using Qiagen RNeasy kit (Hilden, Germany) according
157 to manufacturer protocol. Whole-transcriptome sequencing (RNA-sequencing) was performed

158 using TruSeq™ Stranded Total RNA With Illumina® Ribo-Zero™ Plus rRNA Depletion kit
159 according to manufacturer protocol (Illumina, Inc. San Diego, California). The analysis workflow
160 is in supplemental Methods.

161

162 *CITE-Seq*

163 Two million peripheral blood mononuclear cells (PBMCs) were treated with vehicle, 66 nM Af.
164 CD19 mAb, and 66 nM ABBV-319 for 24 hours in IMDM (12440053, Thermo Fisher Scientific)
165 supplemented with 10% human serum (H4522, Sigma Aldrich). Viable cells were washed and
166 resuspended in cell staining buffer (420201, BioLegend). Following 100 µm strainer filtration,
167 cells were blocked with Fc block (422302, BioLegend) in cell staining buffer and stained with
168 TotalSeq Universal antibody cocktail (399904, BioLegend). Cells were washed and loaded into
169 the 10x Chromium controller at 16,000 cells per sample. Single cell encapsulation was
170 processed according to manufacturer's protocol using 3' chemistry version 3.1 (10X
171 Genomics). Gene expression libraries were sequenced at a depth of 50,000 reads per cell and
172 the surface protein/antibody tag libraries at a depth of 5,000 usable reads per cell on the
173 NextSeq and NovaSeq sequencer (Illumina). The analysis workflow is in supplemental Methods.

174

175 *Immunoblot*

176 Cells were washed twice with ice-cold PBS and then lysed in RIPA lysis buffer (R0278, Sigma-
177 Aldrich) supplemented with 1x Halt™ Protease and Phosphatase Inhibitor Cocktail (78446,
178 Thermo Fisher Scientific). The protein concentrations of the lysates were measured with BCA
179 Protein Assay Kit (23227, Thermo Fisher Scientific). Equal amounts of lysates (1-10 µg) were

180 resolved on 4-12% gradient gels (NW04120BOX, Thermo Fisher Scientific) and transferred onto
181 a PVDF membrane (IB24001, Thermo Fisher Scientific). The membranes were incubated with
182 primary antibodies and secondary antibody conjugated with horseradish peroxidase (HRP).
183 Enhanced chemiluminescent substrates (ECL, Thermo Fisher Scientific) were added and
184 detected with Azure Image Systems C600. Details of immunoblot detection and antibodies used
185 are in supplemental Methods.

186

187 *Glucocorticoid Response Element (GRE) reporter activation assay*

188 50,000 GRE luciferase reporter cells were treated with dose-titrated drugs in growth media
189 containing 1% charcoal stripped FBS (12676-029, Thermo Fisher Scientific) until indicated
190 endpoint. Dual-Glo Luciferase Assay System (E2920, Promega) substrate and buffer were added
191 for 10 minutes and analyzed for luminescence using the MicroBeta (PerkinElmer).

192

193 *In vitro antibody-dependent cellular cytotoxicity (ADCC) assays*

194 The ADCC Reporter Bioassay (G7010 and G9790, Promega) were performed according to the
195 manufacturer's protocol. The target lymphoma cells were labeled with CFSE (C34554, Thermo
196 Fisher Scientific) and then opsonized with antibody or ADC. PBMCs from healthy donors were
197 added at indicated effector to target (E:T) ratios. After 4-hour incubation, cells were stained with
198 Live/Dead Fixable Violet Dead Cell Stain Kit (L34955, Thermo Fisher Scientific) and fixed with 4%
199 paraformaldehyde. The fixed cells were analyzed on Stratadigm S1000EON flow cytometer. The
200 % specific lysis was calculated by subtracting the percentage of dead target cells (% Violet dye+

201 in CFSE+ cells) in each treated condition with the untreated control containing only effector and
202 target cells.

203

204 *In vivo efficacy study*

205 All experiments were conducted in compliance with AbbVie's Institutional Animal Care and Use
206 Committee and the National Institutes of Health Guide for Care and Use of Laboratory Animals
207 guidelines. CDX studies were conducted in-house whereas DLBCL PDX studies were conducted
208 at WuXi AppTec (Suzhou, China). Cell lines were inoculated into the flank of female CB17 SCID or
209 SCID beige mice 6 to 8 weeks of age (Charles River Laboratories) or CD34⁺ PBMC-engrafted NSG-
210 tg(hu-IL15) mice at 18 to 21 weeks of age (The Jackson Laboratory) with 1:1 mixture of S-MEM
211 or HBSS (Fisher Scientific, MA) and Matrigel (BD, Franklin Lakes, NJ). DLBCL PDX tumors (30 mm³
212 tumor slices) were inoculated into the flank of 6- to 8-week-old NOD SCID mice. The DLBCL
213 tumor subtypes (GCB or non-GCB) were determined by immunohistochemical staining for CD10,
214 BCL6 and MUM1.²⁵ Tumors were size matched at approximately 80 to 200 mm³, and the small
215 molecules and biologics (antibody and ADC) were dosed via oral (PO) and intraperitoneal (IP)
216 route of administration, respectively. Tail vein bleeds were taken for PK analysis (supplemental
217 Methods). Measurements of length (L) and width (W) of the tumor were obtained via electronic
218 calipers and volume was calculated according to the following equation: $V = (L \times W^2)/2$. Mice
219 were euthanized when tumor volume reached a maximum of 2,000 mm³ or if animal health was
220 compromised, per institutional guidelines.

221

222 % Tumor growth inhibition (%TGI), % tumor volume change and % tumor growth delay (%TGD)
223 were determined with the equations below:

$$224 \Delta\%TGI \text{ max} = 1 - \left(\frac{\text{Volume of treated group on day X} - \text{Volume of treated group at randomization}}{\text{Volume of control group on day X} - \text{Volume of control group at randomization}} \right) * 100$$

225
226 Δ %TGI max was determined when the difference between treatment and control groups were
227 maximal.

$$228$$
$$229 \text{ \% Tumor volume change} = \left(\frac{\text{Volume of treated group on day X} - \text{Volume of treated group at randomization}}{\text{Volume of treated group at randomization}} \right) * 100$$

230
231 Day X is when vehicle-treated tumors reached 1000 mm³.

$$232$$
$$233 \text{ \% TGD} = \left(\frac{TTE_t - TTE_c}{TTE_c} \right) * 100$$

234 TTE_t and TTE_c are median time periods of treated and control groups to reach tumor volumes of
235 (1 cm³) following onset of treatment.

236
237 All experiments were conducted in compliance with AbbVie's Institutional Animal Care and Use
238 Committee and the National Institutes of Health Guide for Care and Use of Laboratory Animals
239 guidelines.

240
241 **Results**

242 *Generation and characterization of ABBV-319*

243 Transcriptomic analysis showed that *CD19* expression is restricted to a few normal tissues (e.g.,
244 spleen, blood) whereas *NR3C1*, gene encoding GR, is expressed ubiquitously (Figure 1A). In the
245 malignant settings, *CD19* is predominantly expressed in B-cell malignancies such as FL, DLBCL,
246 CLL and Mantle Cell lymphoma (MCL) (Figure 1B), while *NR3C1* is also expressed across B-cell
247 malignancies. Importantly, both *CD19* and *NR3C1* expressions are maintained in DLBCL patients
248 following R-CHOP treatment (Figure 1C).

249
250 ABBV-319 comprises a GRM payload conjugated to an afucosylated CD19 antibody via an
251 alanine-alanine protease cleavable dipeptide linker (Figure 1D). The GRM payload was more
252 potent compared to clinical glucocorticoids (dexamethasone and prednisolone) in
253 glucocorticoid-response element (GRE) reporter and *in vitro* cell proliferation assays in a panel
254 of glucocorticoid-sensitive malignant B-cell cell lines (Figure 1E-F). By comparing the median
255 EC₅₀, the GRM payload was 25 and >300 times more potent compared to dexamethasone and
256 prednisolone, respectively.

257
258 Af. CD19 mAb and ABBV-319 were cross-reactive to both human and cynomolgus monkey CD19
259 (supplemental Figure 1A-E). Twenty-four hour treatment of ABBV-319 on KARPAS422 cells
260 resulted in CD19 internalization and lysosomal trafficking, as shown by the colocalization of
261 CD19 and LysoTracker (Figure 1G). Furthermore, there was dose-dependent activation of GRE
262 reporter activity after ABBV-319 treatment on K562 cells (Figure 1H; supplemental Figure 1D-E),
263 which confirmed the subsequent release of GRM payload in the lysosome followed by induction
264 of GR transcription. ABBV-319 treatment elicited dose-dependent cytotoxicity that was

265 dependent on CD19, as the isotype-GRM ADC showed a significant reduction in activity in SU-
266 DHL-6 (Figure 1I). In the screen of a panel of B-cell malignant cell lines, ABBV-319 showed
267 potent anti-proliferative activity in cell lines across a range of indications including DLBCL, MCL,
268 FL, and ALL (Figure 1J; supplemental Table 2). There was not a significant association between
269 ABBV-319 sensitivity and expression of CD19 or GR (supplemental Figure 2 A-D). B-cell
270 lymphoma with *MYC* and *BCL2* and/or *BCL6* rearrangement are known as double-hit lymphoma
271 (DHL) or triple-hit lymphoma (THL), respectively.²⁶ The DHL and THL are considered as high-
272 grade B-cell lymphoma with inferior survival outcomes when treated with R-CHOP.²⁶⁻²⁸ Notably,
273 several DHL cell lines (DB, OCI-LY19, DoHH-2 and OCI-LY18) with *MYC* plus *BCL2* or *BCL6*
274 rearrangements are still responsive to ABBV-319 (Figure 1J).

275

276 *ABBV-319 engaged and activated GR in DLBCL cell lines*

277 We carried out pharmacodynamic analysis to evaluate the ability of GRM payload to engage
278 endogenous GR in malignant B-cells. GR is phosphorylated on serine 211 (S211) in response to
279 glucocorticoid treatment and this phosphorylation event is required for GR transcriptional
280 activity.^{29,30} Both GRM payload and ABBV-319 treatment elicited a marked increase in S211
281 phosphorylation on GR in Farage, SU-DHL-6 and OCI-LY19 (Figure 2A-C).

282

283 We also performed RNA-seq analysis to characterize the transcriptomic changes in GRM-
284 sensitive cell lines (OCI-LY19, DoHH2, Farage, Pfeiffer, SU-DHL6, OCI-LY3, TMD-8, U-2932)
285 following ABBV-319 treatment. Compared to the vehicle control, ABBV-319 treatment elevated
286 the expression of several reported GR targets (e.g., *TSC22D3*, *DDIT4*, *FKBP5* and *KLF9*) (Figure

287 2D). Moreover, the meta-analysis of the differential expressed genes between ABBV-319
288 treatment versus vehicle control revealed enrichment of gene sets related to
289 steroid/corticosteroid response (Figure 2E).

290
291 To investigate the specificity of ABBV-319, we carried out CITE-seq experiments by treating
292 PMBCs with vehicle, Af. CD19 mAb and ABBV-319. We used a published 8-gene glucocorticoid
293 gene signature³¹ to evaluate the pharmacodynamic effects of ABBV-319 on PBMC. ABBV-319
294 treatment for 24 hours resulted in the most prominent activation of glucocorticoid gene
295 signatures in the B-cell population (Figure 2F-G). Other immune subsets (T, NK, Monocytes)
296 displayed minimal glucocorticoid gene signature activation as compared to the B-cells.
297 Collectively, our data demonstrated that ABBV-319 can specifically deliver GRM payload to
298 CD19+ B-cells and release GRM payloads to activate GR transcriptional activity.

299
300 *ABBV-319 inhibited pro-survival signaling and induces apoptotic cell death*

301 In our *in vitro* screen, some B-cell NHL cell lines (OCI-LY2, TMD-8, Jeko-1, JVM-2, and SU-DHL-6)
302 were sensitive to the unconjugated CD19 mAb (Af. CD19 mAb) treatment (Figure 3A;
303 supplemental Table 2). We hypothesize that Af. CD19 mAb could block BCR-mediated PI3K
304 activation. Indeed, Af. CD19 mAb pre-treatment blunted anti-IgM-stimulated phosphorylation
305 on AKT (S473) (Figure 3B), suggesting that the unconjugated CD19 mAb can block BCR-mediated
306 PI3K pro-survival signaling. Notably, Af. CD19 mAb-mediated signaling effects were not observed
307 in non-responsive cell line SU-DHL-4 (supplemental Figure 3A).

308

309 In the meta-analysis of the RNA-seq data, we found that ABBV-319 elevated expression of genes
310 involved in apoptosis such as *BCL2L11*, *BMF*, and *TXNIP* (Figure 3C). *BCL2L11* encodes BIM and
311 has previously been shown to be involved in glucocorticoid-induced apoptosis.¹³ Consistent with
312 published reports, BIM expression is up-regulated by both GRM and ABBV-319 treatment in
313 Farage, SU-DHL-6 and OCI-LY19 (Figure 3 D-F). Notably, GRM and ABBV-319 treatment led to an
314 increase in all three BIM splice isoforms (BIM_{EL}, BIM_L, BIM_S) that have been shown to be
315 involved in apoptosis.³² The increase in BIM expression also correlated with the increase in
316 cleaved caspase 3, cleaved PARP, and sub-G1 population (dead cells) from the Western blot and
317 flow cytometric analysis (Figure 3D-I). Importantly, these GRM- and ABBV-319 driven apoptotic
318 and cytotoxic effects are specific to the responsive, but not resistant, cell lines (supplemental
319 Figure 3B-C).

320

321 *ABBV-319 elicited potent and durable anti-tumor activity in vivo*

322 In multiple DLBCL and ALL CDX, a single-dose of ABBV-319 induced dose-dependent tumor
323 regression and durable tumor control (Figure 4A-C, E; supplemental Figure 4A-C). In the RS4;11
324 tumor model where tumors were allowed to grow to large sizes (>600mm³), a single-dose of
325 ABBV-319 at 10 mg/kg resulted in durable tumor regression >40 days (Figure 4D), suggesting
326 that ABBV-319 is efficacious in settings that are typically difficult to treat. Remarkably, the anti-
327 tumor activity of a single-dose of ABBV-319 is superior compared to multiple doses (n=15) of
328 prednisolone at 50 mg/kg (the MTD) or multiple doses of GRM (n=15) at 10 mg/kg (Figure 4A-B,
329 4E; supplemental Figure 4C).

330

331 The isotype-GRM ADC, the non-targeting control, displayed marginal anti-tumor activity at 10
332 mg/kg, but to a much lesser extent than the anti-tumor activity observed with ABBV-319 dosed
333 at 10 mg/kg, suggesting a CD19-dependent delivery of GRM to the tumor (Figure 4E;
334 supplemental Figure 4C). Hematological tumor models show higher levels of Fc receptors and
335 thus could potentially result in non-specific uptake of isotype-GRM ADC.

336
337 There was a dose-dependent increase in total antibody concentration and area under the curve,
338 suggesting that ABBV-319 exhibits linear pharmacokinetics in mice (Figure 4F; supplemental
339 Figure 4D). Importantly, the increase in total antibody serum concentration correlated with the
340 anti-tumor activities of ABBV-319. Moreover, the tumor control in OCI-LY19 tumors correlated
341 with the induction of selected GR targets including *FKBP5*, *TSC22D3*, and *ZBTB16* (Figure 4G-H),
342 demonstrating on-target pharmacodynamic effects of GRM *in vivo*.

343
344 ABBV-319 was also tested in DLBCL PDXs to examine its activity in clinically relevant B-cell NHL
345 models. A single-dose of ABBV-319 at 10 mg/kg elicited tumor regression in PDXs that were
346 treatment-naïve or relapsed after 4-7 rounds of R-CHOP treatments (Figure 5A-F). In the PDX
347 study, ABBV-319 elicited tumor growth inhibition compared to the vehicle control in 10/10 PDXs
348 and regression in 9/10 PDXs (Figure 5E). Robust tumor regression induced by ABBV-319 was
349 observed in 7/10 PDXs when the vehicle-treated tumors reached 1000 mm³ (Figure 5F). Similar
350 to our *in vitro* cell line observations, Af. CD19 mAb treatment resulted in tumor growth
351 inhibition in 1/10 DLBCL PDX (Figure 5C).

352

353 *ABBV-319 induced antibody-dependent cellular cytotoxicity in vitro and in vivo*

354 Therapeutic antibodies can elicit anti-tumor activity via Fc-mediated effector functions such as
355 ADCC, antibody-dependent cellular phagocytosis (ADCP), and complement-dependent
356 cytotoxicity (CDC)³³. We first assessed the ability of ABBV-319 to engage ADCP and CDC *in vitro*.
357 The treatment with unconjugated Af. CD19 mAb and ABBV-319 resulted in an increase in
358 macrophage-mediated ADCP in Raji and NU-DHL-1 cells (supplemental Figure 5A-C). Consistent
359 with literature report³⁴, rituximab induced CDC in response to the addition of complements in
360 Raji, Ramos and SU-DHL-6 (supplemental Figure 5D-F). However, neither Af. CD19 mAb nor
361 ABBV-319 showed CDC activity in these experiments. These data therefore demonstrated that
362 ABBV-319 can engage ADCP but not CDC *in vitro*.

363
364 The antibody backbone of ABBV-319 was afucosylated to increase Fc-mediated effector
365 function. Af. CD19 mAb and ABBV-319 induced higher specific lysis of tumor cells compared to
366 their fucosylated counterparts when co-cultured with PBMC (Figure 6A). ABBV-319, and Af.
367 CD19 mAb, also activated NFAT reporter activity with similar potency in Jurkat reporter cells
368 expressing V158 (high affinity) and F158 (low affinity) FcγRIIIa (Figure 6B-C). Moreover, ABBV-
369 319 elicited potent specific lysis of B-cell lymphoma (ALL, BL and DLBCL) cell lines in co-cultured
370 with PBMC (Figure 6D-F). Notably, FcγRIIIa binding and ADCC activity of ABBV-319 were
371 comparable to the Af. CD19 mAb, indicating that conjugation of GRM payloads at DAR4 did not
372 negatively impact ADCC activity.

373

374 Due to the differences in human and mouse FcγR network, humanized mouse models have
375 been developed to better model human NK cell biology³⁵⁻³⁷. In particular, NSG-Tg(Hu-IL15) is a
376 humanized NSG mice that is engineered to express human interleukin 15 (IL-15) at physiological
377 levels, which enables differentiation and development of functional human NK cells after CD34+
378 hematopoietic stem cell (HSC) engraftment³⁷. A single-dose of ABBV-319 at 5 mg/kg elicited
379 deeper tumor growth inhibition and more durable anti-tumor activity in CD34+ PBMC engrafted
380 NSG-Tg(hu-IL15) compared to CB17 SCID mice (Figure 6G). The anti-tumor effects of ABBV-319
381 were dose-dependent and durable tumor regression were observed at the 5 mg/kg dose in OCI-
382 LY19 CDX in NSG-Tg(hu-IL15) (Figure 6H). Notably, flow cytometric immunophenotyping human
383 cells in the periphery showed that ABBV-319 specifically depleted normal human B- but not NK-
384 or T- cells (Figure 6I). The depletion of normal human B-cells is transient, and the peripheral B-
385 cell counts rebound over time. ABBV-319 also elicited superior anti-tumor efficacy compared to
386 Af. CD19 mAb in Raji CDX model in NSG-Tg(hu-IL15) when both agents were dosed at 5 mg/kg
387 (Figure 6J). Collectively, these data demonstrate robust ADCC activity of ABBV-319 and support
388 additive, or synergistic, anti-tumor activities from the combination of different MOAs.

389

390 **Discussion**

391 This is the first study demonstrating the therapeutic potential of a GRM ADC in oncology. Our
392 study demonstrated that ABBV-319 consists of three distinct MOAs that drive anti-tumor
393 activity in B-cell malignancy (Figure 7): (1) delivery of GRM payload via CD19 to activate
394 apoptotic cell death, (2) CD19 downstream signaling inhibition, and (3) enhanced ADCC from
395 afucosylation of the antibody backbone.

396

397 The GRM-mediated anti-tumor activity of ABBV-319 was demonstrated *in vitro* and in immune-
398 compromised mice, in which Af. CD19 mAb showed modest efficacy. This is further supported
399 by the pharmacodynamic analysis showing GR engagement and target gene induction following
400 ABBV-319 treatment. Remarkably, a single-dose of ABBV-319 imparts superior anti-tumor
401 efficacy compared to repeat daily dosing of prednisolone at its MTD *in vivo* (Figure 4A-B, 4E;
402 supplemental Figure 4C). The striking improvement in efficacy is likely attributed to the targeted
403 delivery of a potency-enhanced GRM payload to the CD19+ malignant cells, as well as the PK
404 and safety benefits of improved ADC exposure and lower systemic GRM payload levels relative
405 to the small molecule prednisolone. There was not a significant correlation between ABBV-319
406 sensitivity versus CD19 or GR expression *in vitro*. There are conflicting reports on the correlation
407 of CD19 ADC sensitivity to antigen expression, which may be influenced by the affinity of CD19
408 antibody, potency of the payload and uptake/processing of the ADC.^{38,39} ABBV-319 consists of
409 multiple MOAs that are difficult to model simultaneously *in vitro* and in mouse model systems.
410 Thus, future studies are needed to further define predictive biomarkers for ABBV-319 using
411 clinical datasets.

412

413 A recent functional genomic study reported CD19 is essential for the survival of BL and GCB
414 DLBCL cell lines.²³ In part, this essentiality is driven by BCR-mediated phosphorylation of the
415 YXXM motif on CD19 which can result in recruitment and activation of pro-survival PI3K
416 signaling.¹⁹ Our data demonstrated that Af. CD19 mAb is capable of blocking BCR-mediated PI3K
417 activation (Figure 3B). However, the anti-proliferative activity evoked by Af. CD19 mAb was not

418 restricted to BL or GCB DLBCL as shown in the functional genomic studies.²³ It is conceivable
419 that inhibitory effects of the mAb could be partial compared to complete deletion of the target.
420 Future studies are needed to better understand biomarkers that would predict response to the
421 CD19 antibody-mediated anti-tumor mechanism within ABBV-319.

422
423 Glucocorticoids combine well with chemotherapy and therapeutic antibodies because of their
424 synergistic efficacy and manageable toxicity.⁶ Glucocorticoids are part of the standard-of-care
425 chemo-immunotherapy regimens (i.e., R-CHOP, hyper CVAD, or EPOCH-R) and it is anticipated
426 that ABBV-319 could be a viable combination partner in B-cell malignancies. ABBV-319 showed
427 superior anti-tumor activity compared to the unconjugated Af. CD19 mAb in the immune-
428 competent NSG-tg(hu-IL15) model (Figure 6J), demonstrating that different MOAs of ABBV-319
429 (GRM payload activity, CD19 inhibition, and ADCC) combine optimally to enhance its anti-tumor
430 activity *in vivo*. This is likely due to the ability of GRM payload to induce apoptosis, as
431 mitochondrial apoptosis has been shown to be associated with NK-mediated killing of tumor
432 cells.⁴⁰ Contrary to published reports with systemic glucocorticoids,⁴¹⁻⁴³ the total NK cell
433 numbers were not impacted by ABBV-319 treatment in the NSG-tg(hu-IL15) model,
434 demonstrating that ABBV-319 treatment did not negatively impact NK cell health.

435
436 ABBV-319 displayed remarkable efficacy in clinically relevant B-cell malignancy models. ABBV-
437 319 treatment led to tumor regression and durable tumor control in both non-GCB and GCB
438 DLBCL PDXs, with all models showing sensitivity to the ADC (Figure 5E-F). Non-GCB DLBCL
439 represents a more aggressive disease as it has worse 5-year overall survival compared to GCB

440 DLBCL.²⁵ Furthermore, PDXs with relapsed disease after R-CHOP treatment were still responsive
441 to ABBV-319, suggesting a potential role of ABBV-319 in the R/R setting. Collectively, these
442 positive preclinical data support the ongoing evaluation of ABBV-319's safety, tolerability, and
443 preliminary activity in Phase I clinical trial (NCT05512390).

444

445 **Acknowledgements**

446 We would like to thank Mandy Meng-Shan Wu of AbbVie for their analysis. No further funding
447 to disclose.

448

449 **Author Contributions**

450 **Conception and design:** CAC, EE, AD, WZ, TU, JWP

451 **Acquisition of data:** CAC, AD, CC, DM, EP, AO, PE, LR, CH, LL, WA, PZ, AH, KM, ZZ, GR, ZC, OP, JC

452 **Analysis and interpretation of data (e.g., statistical analysis, biostatistics, computational**

453 **analysis):** CAC, EE, AD, WZ, CC, DM, RD, AH, KM, TU, JWP

454 **Writing, review, and/or revision of the manuscript:** CAC wrote the manuscript and all authors
455 reviewed the manuscript prior to submission.

456

457 **Disclosure of Conflicts of Interest**

458 CAC, EE, ALD, WZ, CC, KP, DM, EP, AO, PE, LR, RD, CH, LL, WA, PZ, WL, AHJ, KM, ZZ, GR, ZC, YL, JC,

459 GZ, TC, MB, CCM, AH, MM, TU, MAP, XZ, JH, MM, KF, SML, and JWP are employees of AbbVie.

460 OP and AB were employees of AbbVie at the time of the study. The design, study conduct, and

461 financial support for this research were provided by AbbVie. AbbVie participated in the
462 interpretation of data, review, and approval of the publication.

463

464 **References**

- 465 1. Thandra KC, Barsouk A, Saginala K, Padala SA, Barsouk A, Rawla P. Epidemiology of Non-
466 Hodgkin's Lymphoma. *Med Sci (Basel)*. 2021;9(1).
- 467 2. Shadman M. Diagnosis and Treatment of Chronic Lymphocytic Leukemia: A Review. *JAMA*.
468 2023;329(11):918-932.
- 469 3. Armitage JO, Gascoyne RD, Lunning MA, Cavalli F. Non-Hodgkin lymphoma. *Lancet*.
470 2017;390(10091):298-310.
- 471 4. Sehn LH, Salles G. Diffuse Large B-Cell Lymphoma. *N Engl J Med*. 2021;384(9):842-858.
- 472 5. Peyrade F, Jardin F, Thieblemont C, et al. Attenuated immunochemotherapy regimen (R-
473 miniCHOP) in elderly patients older than 80 years with diffuse large B-cell lymphoma: a multicentre,
474 single-arm, phase 2 trial. *Lancet Oncol*. 2011;12(5):460-468.
- 475 6. R. B. Livingston SKC. Single Agents in Cancer Chemotherapy. New York, NY: Springer 1970.
- 476 7. Pearson OH, Eliel LP. Use of pituitary adrenocorticotrophic hormone (ACTH) and cortisone in
477 lymphomas and leukemias. *J Am Med Assoc*. 1950;144(16):1349-1353.
- 478 8. Kofman S, Perlia CP, Boesen E, Eisenstein R, Taylor SG, 3rd. The role of corticosteroids in the
479 treatment of malignant lymphomas. *Cancer*. 1962;15:338-345.
- 480 9. Fisher RI, Gaynor ER, Dahlborg S, et al. Comparison of a standard regimen (CHOP) with three
481 intensive chemotherapy regimens for advanced non-Hodgkin's lymphoma. *N Engl J Med*.
482 1993;328(14):1002-1006.
- 483 10. . !!! INVALID CITATION !!! 10,11.
- 484 11. Weikum ER, Knuesel MT, Ortlund EA, Yamamoto KR. Glucocorticoid receptor control of
485 transcription: precision and plasticity via allostery. *Nat Rev Mol Cell Biol*. 2017;18(3):159-174.
- 486 12. Pufall MA. Glucocorticoids and Cancer. *Adv Exp Med Biol*. 2015;872:315-333.
- 487 13. Ploner C, Rainer J, Niederegger H, et al. The BCL2 rheostat in glucocorticoid-induced apoptosis of
488 acute lymphoblastic leukemia. *Leukemia*. 2008;22(2):370-377.
- 489 14. Rhee K, Bresnahan W, Hirai A, Hirai M, Thompson EA. c-Myc and cyclin D3 (CcnD3) genes are
490 independent targets for glucocorticoid inhibition of lymphoid cell proliferation. *Cancer Res*.
491 1995;55(18):4188-4195.
- 492 15. Oray M, Abu Samra K, Ebrahimiadib N, Meese H, Foster CS. Long-term side effects of
493 glucocorticoids. *Expert Opin Drug Saf*. 2016;15(4):457-465.
- 494 16. Scheuermann RH, Racila E. CD19 antigen in leukemia and lymphoma diagnosis and
495 immunotherapy. *Leuk Lymphoma*. 1995;18(5-6):385-397.
- 496 17. Tedder TF, Inaoki M, Sato S. The CD19–CD21 Complex Regulates Signal Transduction Thresholds
497 Governing Humoral Immunity and Autoimmunity. *Immunity*. 1997;6(2):107-118.
- 498 18. Burger JA, Wiestner A. Targeting B cell receptor signalling in cancer: preclinical and clinical
499 advances. *Nat Rev Cancer*. 2018;18(3):148-167.
- 500 19. Tuveson DA, Carter RH, Soltoff SP, Fearon DT. CD19 of B cells as a surrogate kinase insert region
501 to bind phosphatidylinositol 3-kinase. *Science*. 1993;260(5110):986-989.
- 502 20. Kimura M, Yamaguchi M, Nakamura S, et al. Clinicopathologic significance of loss of CD19
503 expression in diffuse large B-cell lymphoma. *Int J Hematol*. 2007;85(1):41-48.
- 504 21. Johnson NA, Boyle M, Bashashati A, et al. Diffuse large B-cell lymphoma: reduced CD20
505 expression is associated with an inferior survival. *Blood*. 2009;113(16):3773-3780.
- 506 22. Xu X, Sun Q, Liang X, et al. Mechanisms of Relapse After CD19 CAR T-Cell Therapy for Acute
507 Lymphoblastic Leukemia and Its Prevention and Treatment Strategies. *Front Immunol*. 2019;10:2664.
- 508 23. Phelan JD, Young RM, Webster DE, et al. A multiprotein supercomplex controlling oncogenic
509 signalling in lymphoma. *Nature*. 2018;560(7718):387-391.
- 510 24. Hammer O. CD19 as an attractive target for antibody-based therapy. *MAbs*. 2012;4(5):571-577.

- 511 25. Hans CP, Weisenburger DD, Greiner TC, et al. Confirmation of the molecular classification of
512 diffuse large B-cell lymphoma by immunohistochemistry using a tissue microarray. *Blood*.
513 2004;103(1):275-282.
- 514 26. Rosenthal A, Younes A. High grade B-cell lymphoma with rearrangements of MYC and BCL2
515 and/or BCL6: Double hit and triple hit lymphomas and double expressing lymphoma. *Blood Rev*.
516 2017;31(2):37-42.
- 517 27. Johnson NA, Savage KJ, Ludkovski O, et al. Lymphomas with concurrent BCL2 and MYC
518 translocations: the critical factors associated with survival. *Blood*. 2009;114(11):2273-2279.
- 519 28. Johnson NA, Slack GW, Savage KJ, et al. Concurrent expression of MYC and BCL2 in diffuse large
520 B-cell lymphoma treated with rituximab plus cyclophosphamide, doxorubicin, vincristine, and
521 prednisone. *J Clin Oncol*. 2012;30(28):3452-3459.
- 522 29. Wang Z, Frederick J, Garabedian MJ. Deciphering the phosphorylation "code" of the
523 glucocorticoid receptor in vivo. *J Biol Chem*. 2002;277(29):26573-26580.
- 524 30. Miller AL, Webb MS, Copik AJ, et al. p38 Mitogen-activated protein kinase (MAPK) is a key
525 mediator in glucocorticoid-induced apoptosis of lymphoid cells: correlation between p38 MAPK
526 activation and site-specific phosphorylation of the human glucocorticoid receptor at serine 211. *Mol*
527 *Endocrinol*. 2005;19(6):1569-1583.
- 528 31. Hu Y, Carman JA, Holloway D, et al. Development of a Molecular Signature to Monitor
529 Pharmacodynamic Responses Mediated by In Vivo Administration of Glucocorticoids. *Arthritis*
530 *Rheumatol*. 2018;70(8):1331-1342.
- 531 32. O'Connor L, Strasser A, O'Reilly LA, et al. Bim: a novel member of the Bcl-2 family that promotes
532 apoptosis. *EMBO J*. 1998;17(2):384-395.
- 533 33. Goydel RS, Rader C. Antibody-based cancer therapy. *Oncogene*. 2021;40(21):3655-3664.
- 534 34. van Meerten T, van Rijn RS, Hol S, Hagenbeek A, Ebeling SB. Complement-induced cell death by
535 rituximab depends on CD20 expression level and acts complementary to antibody-dependent cellular
536 cytotoxicity. *Clin Cancer Res*. 2006;12(13):4027-4035.
- 537 35. Casey E, Bournazos S, Mo G, et al. A new mouse expressing human Fcγ receptors to better
538 predict therapeutic efficacy of human anti-cancer antibodies. *Leukemia*. 2018;32(2):547-549.
- 539 36. Nimmerjahn F, Ravetch JV. Fcγ receptors as regulators of immune responses. *Nat Rev*
540 *Immunol*. 2008;8(1):34-47.
- 541 37. Aryee KE, Burzenski LM, Yao LC, et al. Enhanced development of functional human NK cells in
542 NOD-scid-IL2rg(null) mice expressing human IL15. *FASEB J*. 2022;36(9):e22476.
- 543 38. Ryan MC, Palanca-Wessels MC, Schimpf B, et al. Therapeutic potential of SGN-CD19B, a PBD-
544 based anti-CD19 drug conjugate, for treatment of B-cell malignancies. *Blood*. 2017;130(18):2018-2026.
- 545 39. Zammarchi F, Corbett S, Adams L, et al. ADCT-402, a PBD dimer-containing antibody drug
546 conjugate targeting CD19-expressing malignancies. *Blood*. 2018;131(10):1094-1105.
- 547 40. Pan R, Ryan J, Pan D, Wucherpfennig KW, Letai A. Augmenting NK cell-based immunotherapy by
548 targeting mitochondrial apoptosis. *Cell*. 2022;185(9):1521-1538 e1518.
- 549 41. Rose AL, Smith BE, Maloney DG. Glucocorticoids and rituximab in vitro: synergistic direct
550 antiproliferative and apoptotic effects. *Blood*. 2002;100(5):1765-1773.
- 551 42. Gatti G, Cavallo R, Sartori ML, et al. Inhibition by cortisol of human natural killer (NK) cell activity.
552 *J Steroid Biochem*. 1987;26(1):49-58.
- 553 43. Pedersen BK, Beyer JM. Characterization of the in vitro effects of glucocorticosteroids on NK cell
554 activity. *Allergy*. 1986;41(3):220-224.
- 555 44. Drexler HG, Eberth S, Nagel S, MacLeod RA. Malignant hematopoietic cell lines: in vitro models
556 for double-hit B-cell lymphomas. *Leuk Lymphoma*. 2016;57(5):1015-1020.

557

558 **Figure Legends**

559 **Figure 1. Characterization of ABBV-319.** (A) Analysis of *CD19* and *NR3C1* gene expression in
560 normal tissues using GTEx datasets. (B) Analysis of *CD19* and *NR3C1* gene expression across
561 different cancer indications using Aster (ORIEN) datasets. (C) Analysis of *CD19* and *NR3C1* gene
562 expression in patients that are treatment-naive or post-R-CHOP treatment using Aster (ORIEN)
563 datasets. Statistical analysis with Wilcoxon's test. ns, not significant. (D) Structure of the
564 glucocorticoid receptor modulator (GRM) linker drug. (E) The fold change in glucocorticoid
565 response element (GRE) activity compared to the untreated control after treatment of K562
566 GRE reporter cells with prednisolone, dexamethasone and GRM payload for 24 hours. Mean \pm
567 SEM are depicted. (F) Summary of EC_{50} for prednisolone, dexamethasone and GRM payload
568 across 20 glucocorticoid-sensitive cell lines. Each dot represents $\log(EC_{50})$ of a cell line and the
569 median $\log(EC_{50})$ is displayed. (G) Imaging analysis of CD19 localization after treatment of
570 KARPAS422 with an Alexa Fluor 647-labeled ABBV-319 for the indicated time. Brightfield,
571 LysoTracker (green), CD19 (red), and merged images are displayed. (H) The fold change in GRE
572 activity relative to the untreated control after treating K562-GRE reporter cells with ABBV-319
573 for 24 hours. (I) % viability of SU-DHL-6 cells relative to the untreated control after treatment
574 with GRM payload, isotype-GRM ADC, and ABBV-319 for 5 days. (J) EC_{50} of ABBV-319 across a
575 panel of malignant B-cell lines with a range of E_{max} from supplemental Table 2. # denotes
576 double-hit lymphoma (DHL) and * denotes triple-hit lymphoma (THL) based on published
577 annotations.⁴⁴
578

579 **Figure 2. ABBV-319 engages and activates GR in DLBCL cell lines.** (A-C) Immunoblot analysis of
580 GR phosphorylation on Serine 211 and GR expression after treatment with 10 nM GRM and 100
581 nM ABBV-319 for indicated time in Farage (A), SU-DHL-6 (B), and OCI-LY19 (C). β -actin was used
582 as the loading control. (D) Volcano plot showing the fold change and p-value from the meta-
583 analysis of differential expressed genes (DEGs) between 24-hour ABBV-319 treatment and
584 vehicle control in GRM-sensitive cell lines. Each dot represents a DEG and selected known GR
585 targets are highlighted in red. (E) Pathways and genes enriched in the meta-analysis of the
586 DEGs between ABBV-319 and vehicle treatment. The color represents directionality of fold
587 change, and the size of circle represents $\log(p\text{-value})$. (F) Heatmap showing the expression of
588 the 8-gene glucocorticoid gene signature in different immune subsets in PMBC after 24-hour of
589 indicated treatment. (G) UMAP projection of the immune cells within PMBC after indicated
590 treatment for 24 hours. The color indicates the expression of the 8-gene glucocorticoid gene
591 signature.
592

593 **Figure 3. ABBV-319 inhibits pro-survival signaling and induces apoptotic cell death in DLBCL.**
594 (A) The % viability relative to the untreated control after the treatment of SU-DHL-6 cells with
595 afucosylated (Af.) isotype mAb and Af. CD19 mAb. Mean \pm SEM are displayed. (B) SU-DHL-6
596 cells were pre-treated with 100 nM Af. Isotype mAb or Af. CD19 mAb for an hour and then
597 stimulated with 1 μ g/ml anti-IgM for indicated time. Cell lysates were resolved on SDS-PAGE
598 and immunoblot analysis for phospho-AKT (Ser473) and GAPDH are displayed. GAPDH is used
599 as the loading control. (C) Volcano plot showing the fold change and p-value from the meta-
600 analysis of differential expressed genes (DEGs) between 24-hour ABBV-319 treatment and

601 vehicle control in ABBV-319-sensitive cell lines. Each dot represents a DEG and genes involved
602 in apoptosis are highlighted in red. (D-F) Immunoblot analysis of BIM, caspase 3, PARP and
603 GAPDH after treating Farage (D), SU-DHL-6 (E) and OCI-LY19 (F) with 10 nM GRM payload and
604 100 nM ABBV-319 for indicated time. The arrows show the cleaved product of caspase 3 and
605 PARP. (G-I) Cell cycle analysis of Farage (G), SU-DHL-6 (H) and OCI-LY19 (I) after treatment with
606 10 nM GRM and 100 nM ABBV-319 for indicated time. The % of cells from sub-G1, G0-G1, S and
607 G2-M phases of cell cycle are displayed.
608

609 **Figure 4. ABBV-319 elicits potent and durable anti-tumor activity in cell line-derived xenograft**
610 **(CDX) models.** (A-E) Growth of xenografted KARPAS422 (A), DB (B), RS4;11 (C-D), OCI-LY19 (E)
611 tumors after the indicated treatment regimen. Drug treatments were initiated within 24-hour
612 after tumor size matching and randomization (A-C, E) whereas the large RS4;11 tumor (D) was
613 dosed at day 43 after inoculation. QD denotes once daily, and SD denotes single dose. Means \pm
614 SEM of tumor volumes were plotted for each treatment group versus days from randomization
615 or days post inoculation. (F) Total antibody detected in mouse whole blood from the OCI-LY19
616 study (E). Means \pm SEM are shown. (G) The volume of xenografted OCI-LY19 tumors after
617 indicated treatment for 7 days. GRM was dosed at (QDx5)x3 whereas ABBV-319 was dosed SD.
618 Means \pm SEM of tumor volumes were plotted for each treatment group. QD denotes once daily,
619 and SD denotes single dose. (H) RT-qPCR analysis of *FKBP5*, *TSC22D3* and *ZBTB16* expression in
620 tumors after indicated treatments. Means \pm SEM of fold change relative to vehicle control are
621 displayed.
622

623 **Figure 5. ABBV-319 exhibits anti-tumor activity in non-GCB DLBCL and relapsed DLBCL**
624 **patient-derived xenograft (PDX) models.** (A-D) The growth of xenografted PDX models 0395
625 (A), 0262 (B), 0207 (C), and 0016 (D) in NOD-SCID mice after indicated treatment regimen.
626 Means \pm SEM of tumor volumes were plotted for each treatment group versus days from
627 randomization. SD denotes single dose. (A) and 0262 (B) were treatment naïve whereas PDX
628 models 0207 (C) and 0016 (D) were from relapsed disease following 4 R-CHOP treatments. GCB
629 and non-GCB subtyping were determined via IHC methods as described in the Methods. (E)
630 Maximal % tumor growth inhibition relative to vehicle control in each PDX model is displayed.
631 Models showing tumor regression after ABBV-319 treatment are shown on the figure. (F) %
632 tumor volume changes relative to the starting tumor volume when the vehicle control reaches
633 1000 mm³. GCB and non-GCB DLBCL are shown as different colors. * denotes PDX samples from
634 patients with relapse disease after R-CHOP treatment.
635

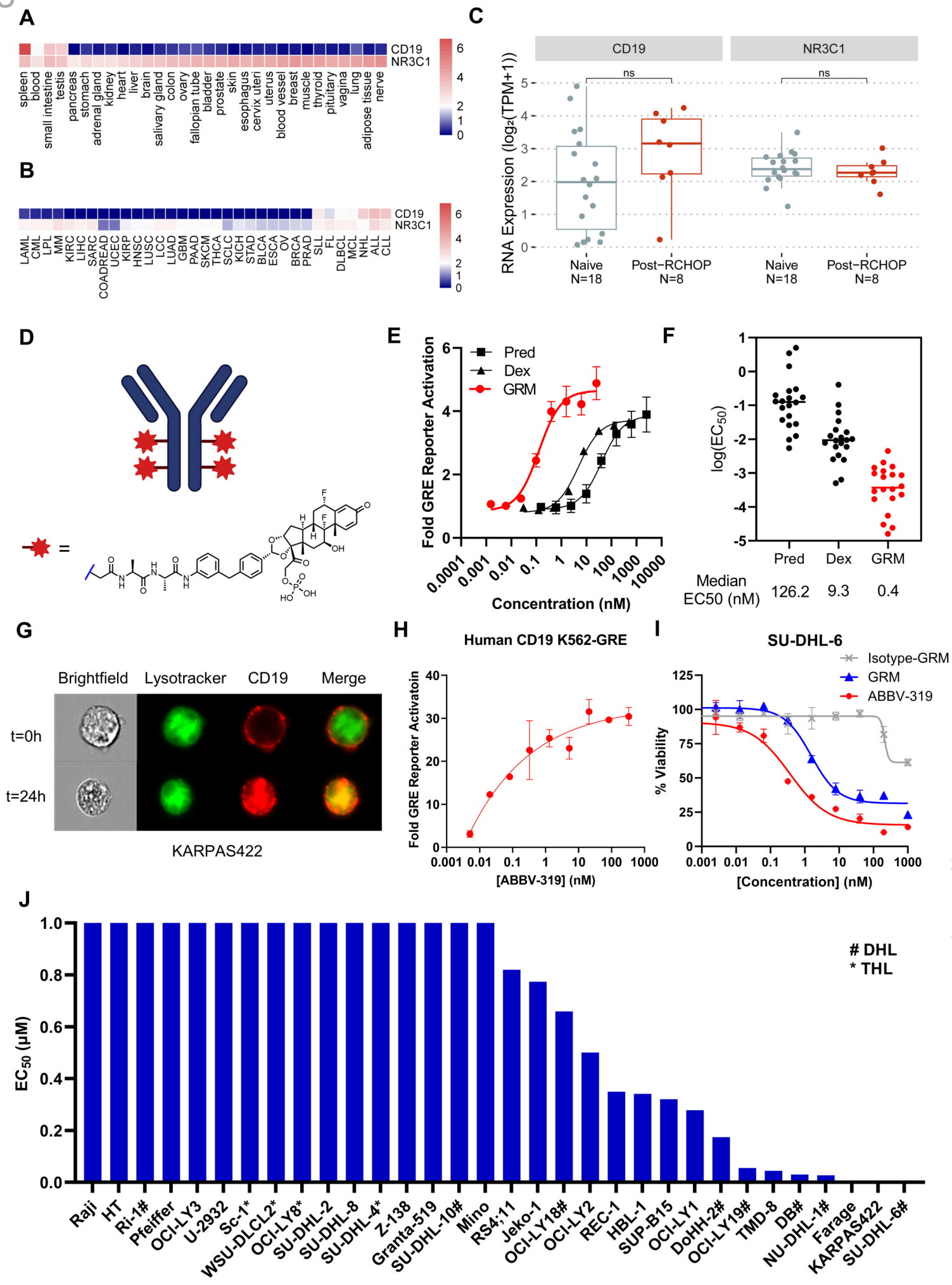
636 **Figure 6. ABBV-319 induces antibody-dependent cellular cytotoxicity (ADCC) *in vitro* and *in***
637 ***vivo*.** (A) % specific lysis of RS4;11 cells in co-culture with PBMC at effector to target (E:T) ratio
638 of 20:1 after 4-hour treatment with indicated agents. Mean \pm SEM are displayed. (B-C)
639 Luciferase reporter activation in Jurkat cells expressing V158 (B) and F158 (C) FcγRIIIa after
640 treatment with indicated agents for 4 and 16 hours, respectively. Mean \pm SEM are displayed.
641 (D-F) % specific lysis of RS4;11 (D), Raji (E), and KARPAS422 (F) in co-culturing with PBMC at E:T
642 ratio of 20:1 after treatment with indicated agent for 4 hours. Mean \pm SEM are displayed. (G)
643 Growth of OCI-LY19 tumors in CB17 SCID or CD34+ PBMC engrafted NSG-tg(hu-IL15) mice after
644 treatment with vehicle or single-dose ABBV-319 at 5 mg/kg. Mean \pm SEM of tumor volumes

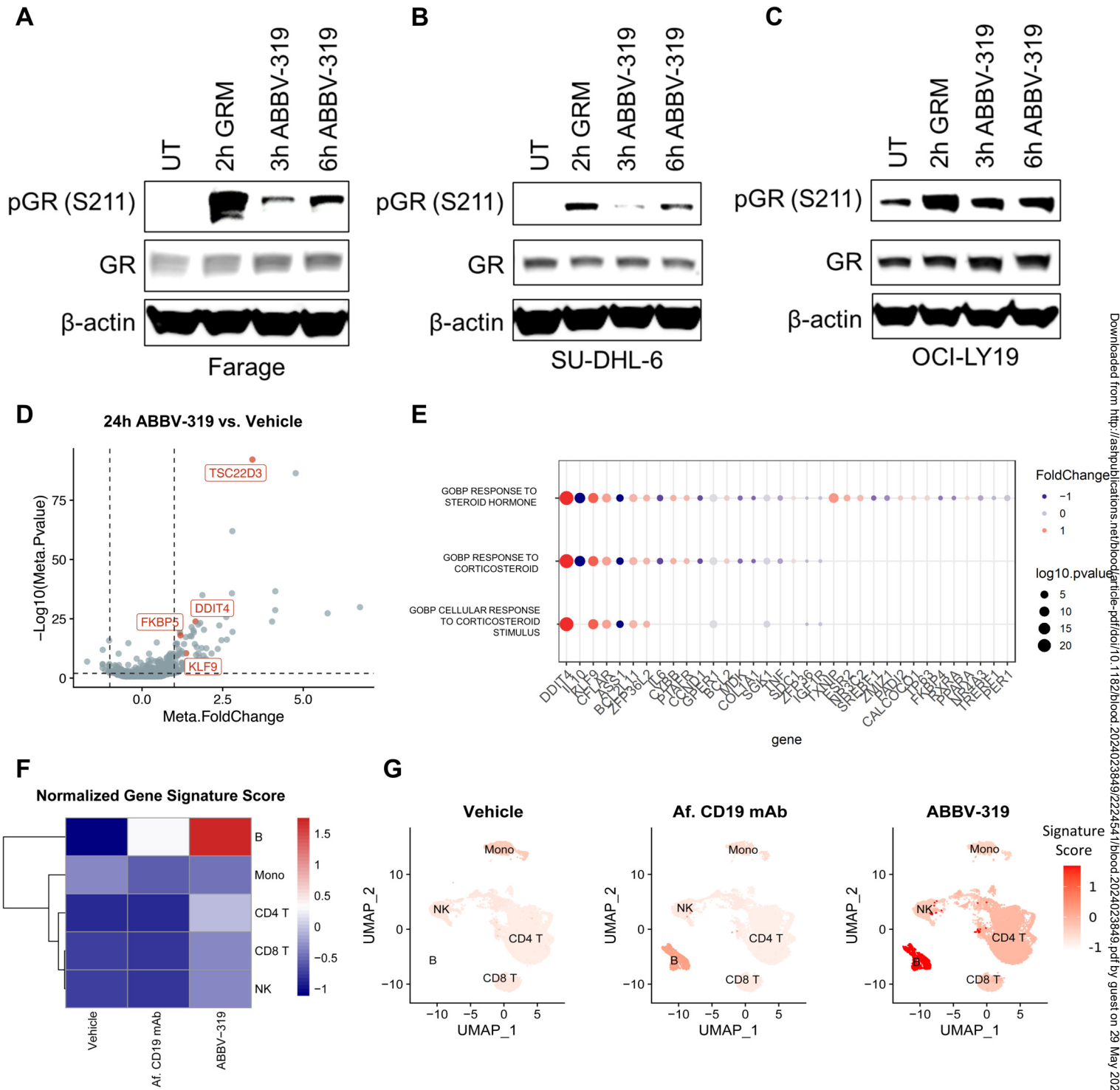
645 were plotted for each treatment group versus days from randomization. ΔTGI_{max} and TGD_{1000}
646 were calculated as described in the Methods. (H) Growth of OCI-LY19 tumors in CD34+ PBMC
647 engrafted NSG-tg(hu-IL15) mice after treatment with vehicle or single-dose of ABBV-319 at 0.5,
648 1.5, and 5 mg/kg. Means \pm SEM of tumor volumes were plotted for each treatment group
649 versus days from randomization. (I) Flow cytometric immunophenotyping analysis of tail vein
650 bleeds from OCI-LY19 tumor bearing mice (H). B cells were presented as the % of CD45+ cells
651 while T and NK cells were presented as % of CD45+ cells without B-cells. Details of the
652 immunophenotyping methods are in supplemental Methods. (J) Growth of Raji tumors in
653 CD34+ PMBC engrafted NSG-tg(hu-IL15) mice after indicated treatment regimen. Means \pm SEM
654 of tumor volumes were plotted for each treatment group versus days from randomization.
655

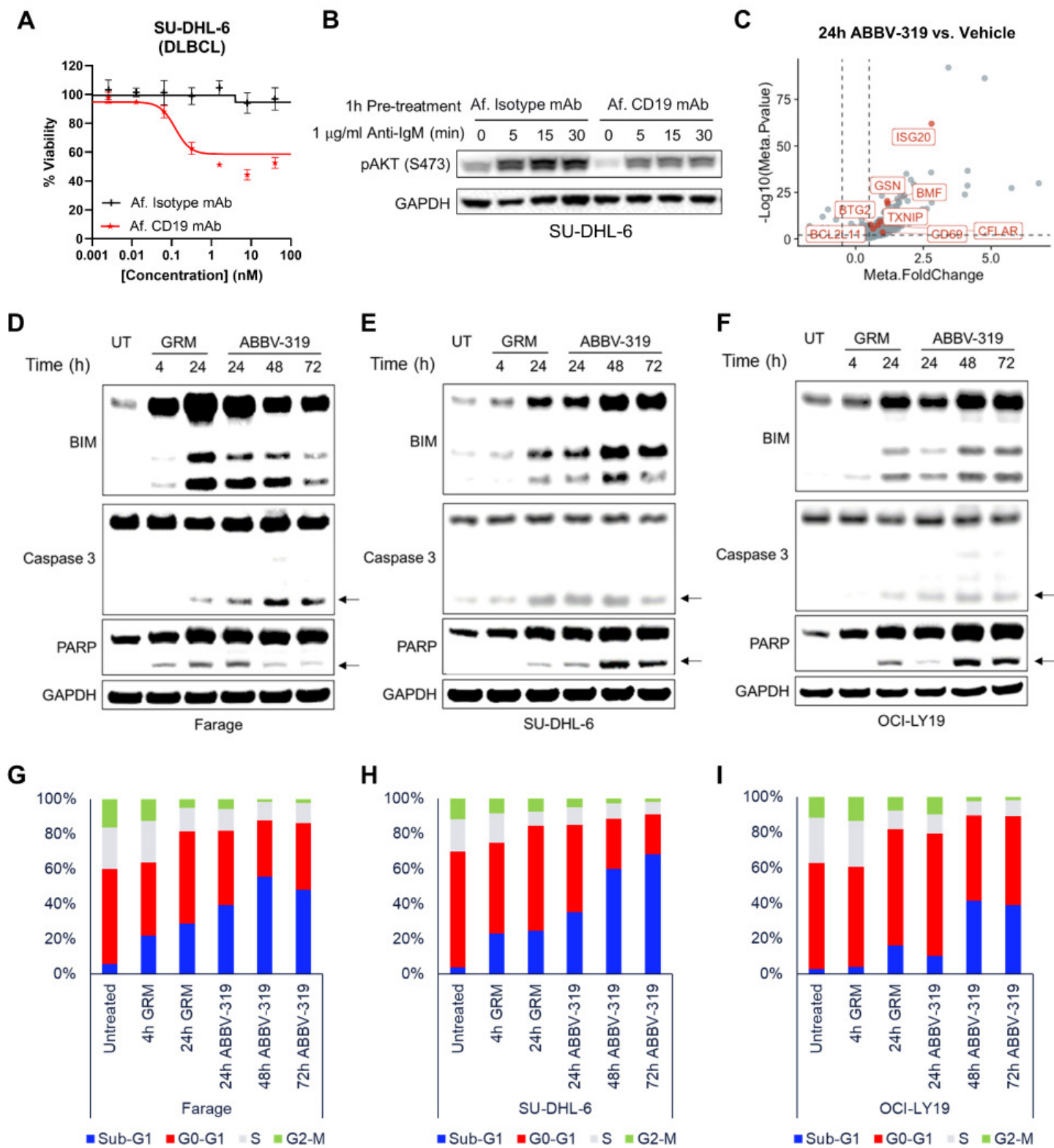
656 **Figure 7. ABBV-319 elicits anti-tumor effects through three distinct mechanisms of action.**

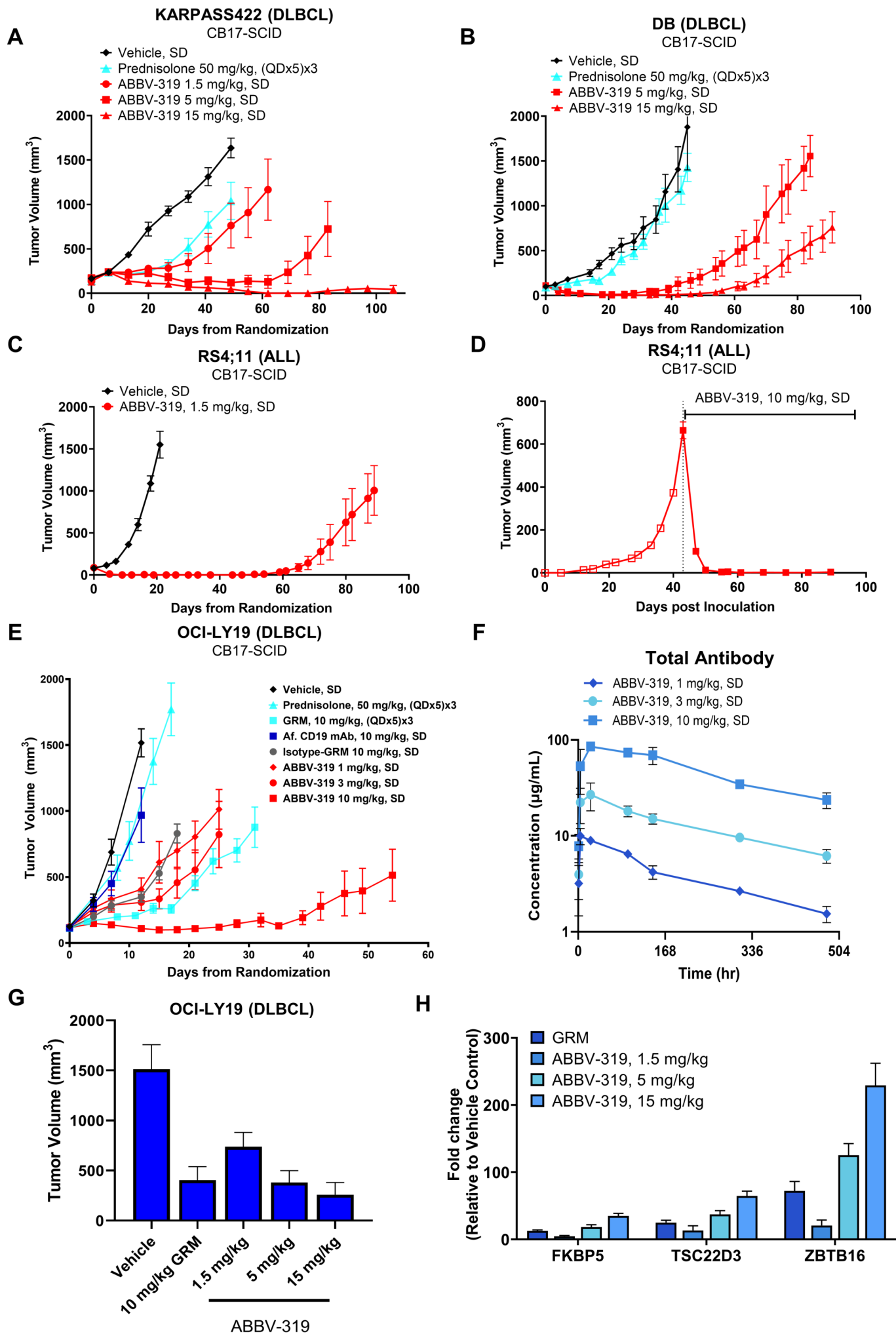
657 ABBV-319 results in CD19 internalization and lysosomal trafficking to release the GRM payload.
658 GRM payload drives transcriptional activation of GR targets (e.g., *BCL2L11*) to activate apoptotic
659 cell death. ABBV-319 also blocks CD19-mediated activation of PI3K pathway. Lastly,
660 afucosylation of the fragment crystallizable (Fc) region enhances ADCC driven by effector cells.
661

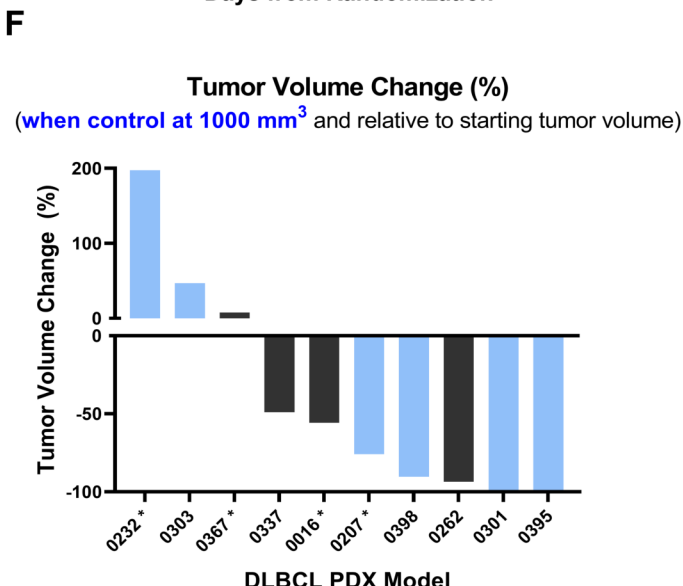
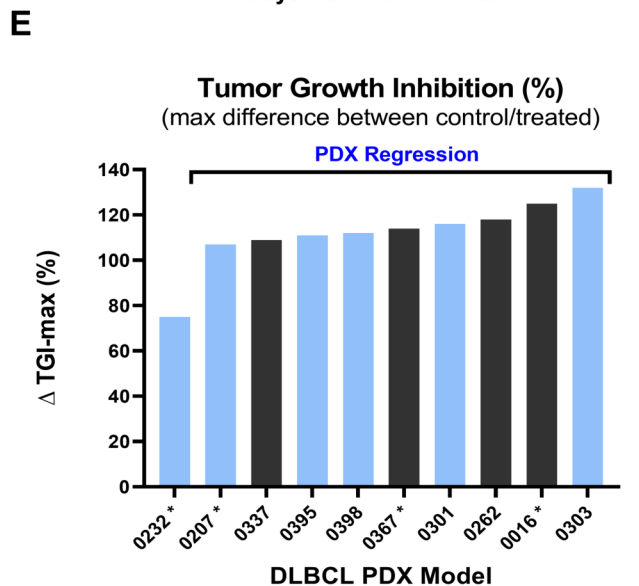
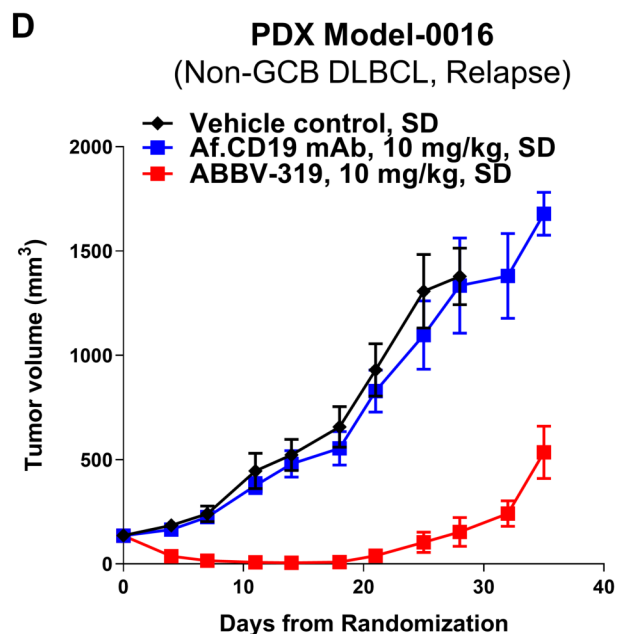
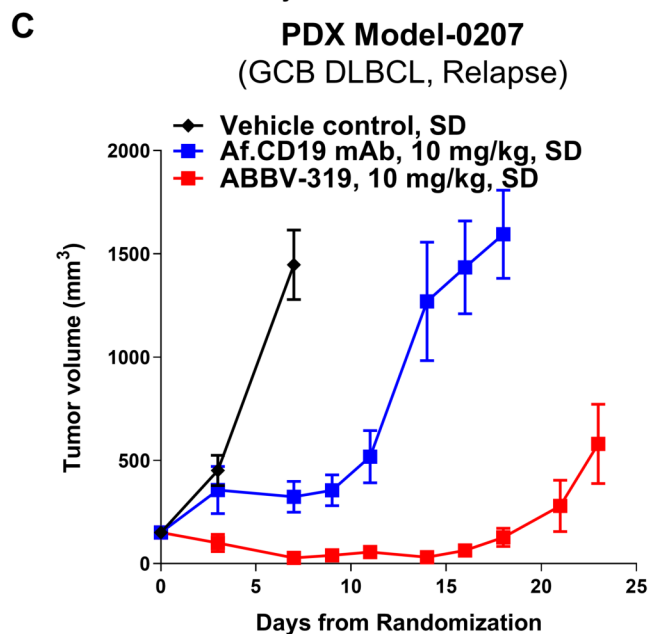
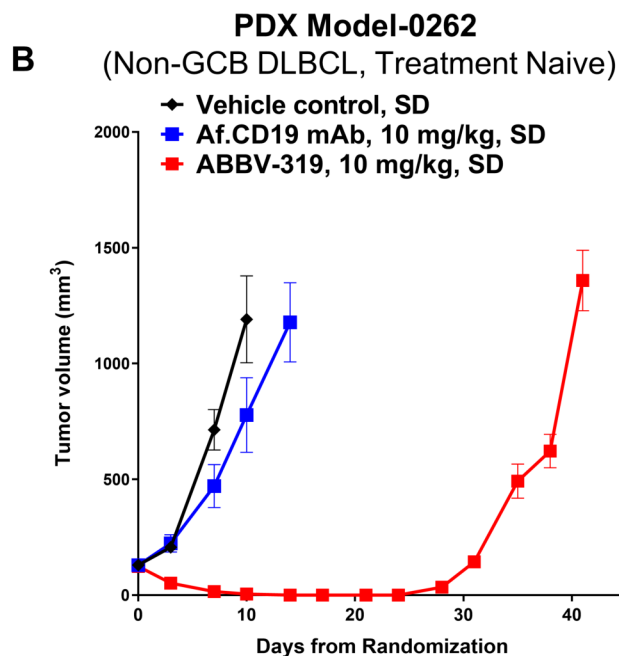
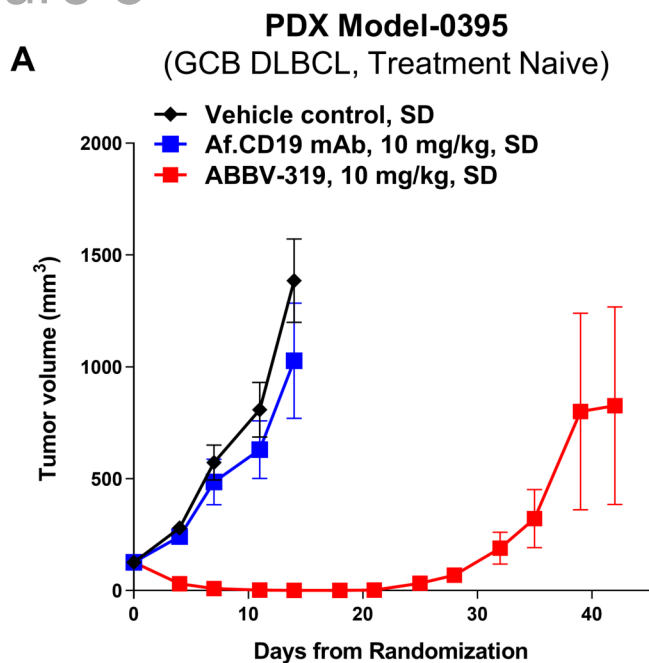
Figure 1











■ GCB

■ Non-GCB

* Relapse after R-CHOP

■ GCB

■ Non-GCB

* Relapse after R-CHOP

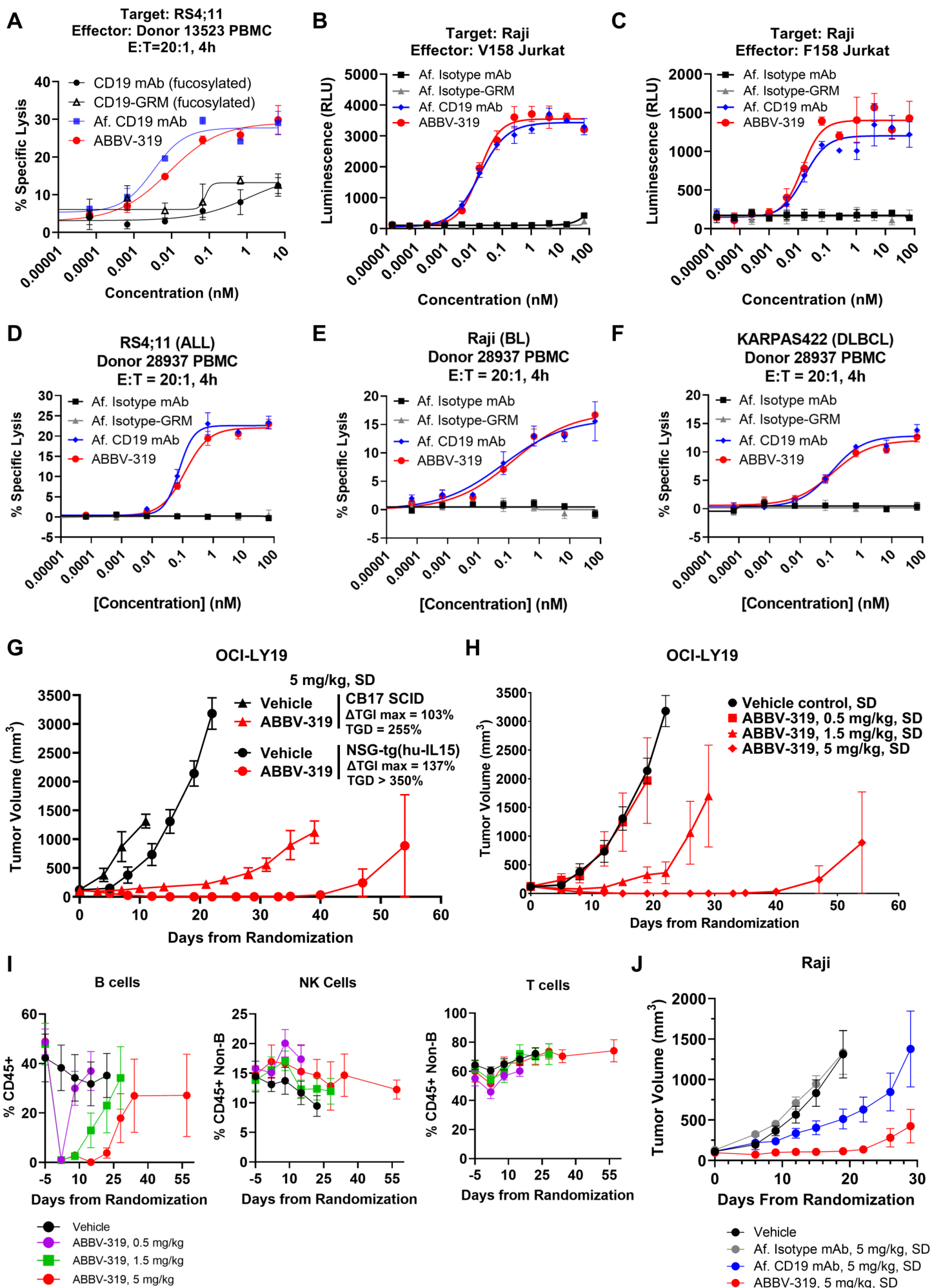
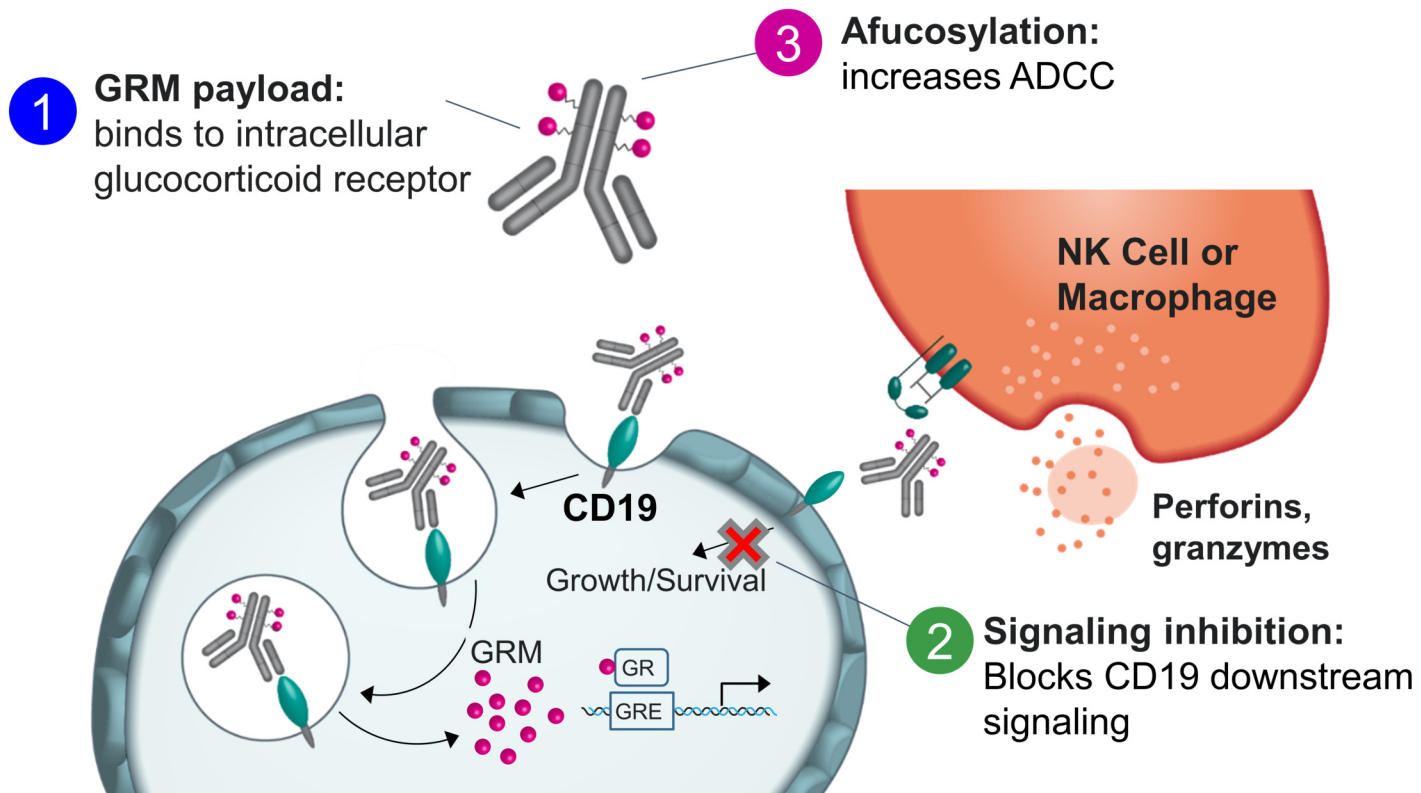
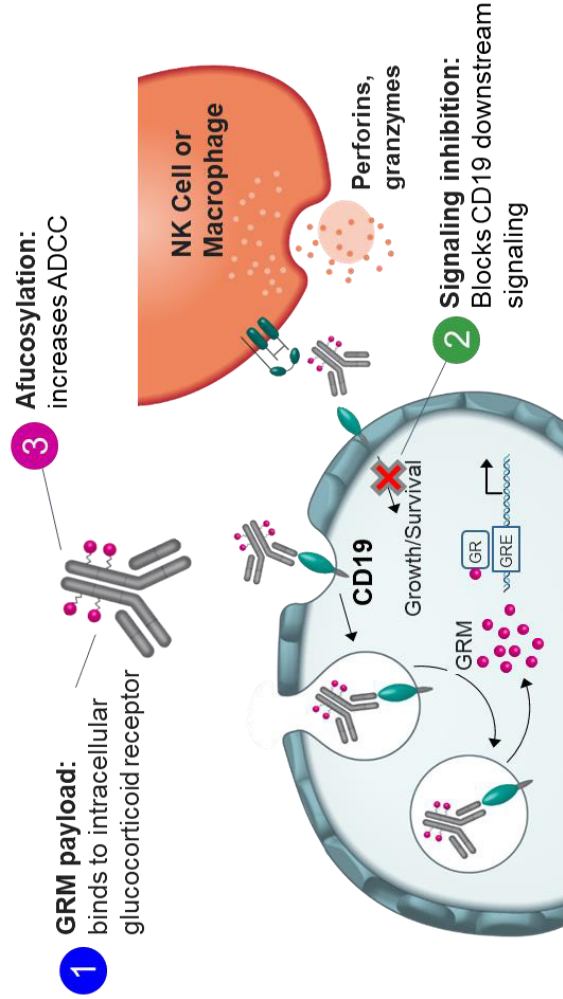


Figure 7

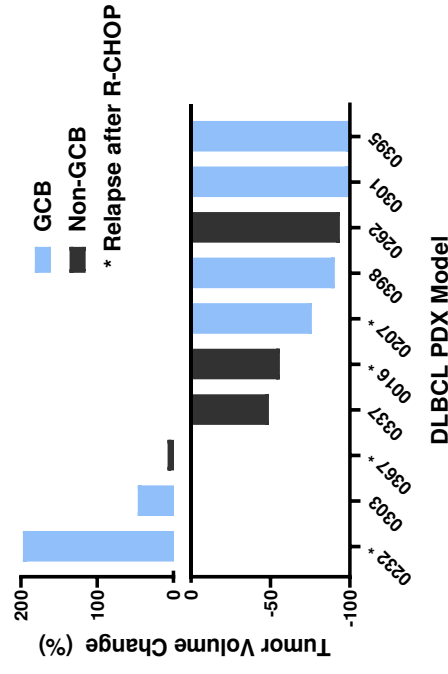


ABBV-319: A Glucocorticoid Receptor Modulator (GRM) Antibody-Drug Conjugate (ADC) For the Treatment of B-cell Malignancies

In this study, ABBV-319 was investigated as a potential treatment for B-cell malignancies.



DLBCL PDX Tumor Volume Change (%)
(when control at 1000 mm³ and relative to starting tumor volume)



ABBV-319 possesses three main mechanisms of action (MOAs) including 1) GRM payload delivery, 2) CD19 signaling inhibition, 3) Enhanced ADCC via afucosylation. Collectively, these MOAs contribute to pronounced anti-tumor activity across B-cell malignancy models.